

# **SIMULATION OF OPEN CIRCUIT VOLTAGE DECAY FOR SOLAR CELL DETERMINATION OF THE BASE MINORITY CARRIER LIFETIME AND THE BACK SURFACE RECOMBINATION VELOCITY**

**B. AFFOUR\* AND P. MIALHE**

*Centre d'Etudes Fondamentales, Université de Perpignan, 52, Avenue de Villeneuve,  
66860 Perpignan, France*

*(Received January 24 1996; In final form March 29 1996)*

The Open Circuit Voltage Decay (OCVD) method for the determination of the base minority carrier lifetime ( $\tau$ ) and the back surface recombination velocity ( $S$ ) of silicon solar cells has been investigated at constant illumination level. The validity of the method has been discussed through a simulation study by considering the mathematical solution of the continuity equation. Extracted values of  $\tau$  and  $S$  are compared to their input values in order to evaluate the performances of our method and the precision with regard to cell structural parameters, namely the base width and the base doping level. Deviations in lifetime values remain lower than 7% for almost all the cell configurations while recombination velocity deviations are shown to be dependent on cell structure parameters and experimental procedure.

## **INTRODUCTION**

In recent years, theoretical works have shown that energy conversion efficiencies of silicon solar cells should be increased by using new cell structures. These cells offer [1] the potential for high efficiencies if light trapping [2] is incorporated to offset the weak absorption. The highest open circuit voltage has been obtained [3] with bifacially contacted  $n^+p$  cells where contact on the p-type substrate is made via small openings in the rear surface. The general trend was to reduce the recombination loss by limiting the silicon-metal interface area. The increase of efficiency with light concentration operating conditions [4] has shown to be limited by saturation effects and by a large increase of the space charge recombination current. A general optimization of the cell performances [5,6] has pointed out the sensitive effect of the base doping level and the back surface recombination velocity for thin cell structures. For these structures, the open circuit voltage and the short circuit current are maximized but the cell fill factor is reduced. Evaluations of the energy loss by the photogenerated carriers in the bulk and at the back surface are an indispensable tool for obtaining an improved knowledge of internal physical processes. This may be done with the measurements of the carrier lifetime and the

---

\*Corresponding author.

back surface recombination velocities which provide [7] a clear vision of the cell structure quality and a quantitative information on the layer degradations.

Experimental methods to determine the carrier lifetime ( $\tau$ ) and the surface recombination velocity ( $S$ ) are based on modelling of a cell transient response obtained either in open circuit or short circuit conditions. For these methods [8], a steady state is abruptly terminated and the transient response is measured. It is well known that the values of the carrier lifetime determined by different experimental methods are not the same. The results differ with the excitation used to obtain the steady state (applied bias or variation of the illumination level) and the experimental conditions affect the decay curve [9,10]. Furthermore, the accuracy in the determination of  $\tau$  and  $S$  is [11] critically dependent on the knowledge of the cell structural parameters.

Since recombination processes are dependent on carrier concentrations, it has been recognized that such measurements must be performed under actual illumination levels. Then, an improvement of the short circuit current decay method has been suggested [12] with operating cells at constant illumination level and no power supply requirement. This experimental procedure has been discussed and applied to commercial cells under normal operating conditions [12,13]. The necessity of a precise knowledge of the structural cell parameters has been shown to impose a limitation of the practical use of short circuit current decay methods.

For the sake of accurate measurements, more insight into the transient decay behavior of the solar cell is required. Numerical modelling is a means to obtain such improved insight, as it allows the determination of the effect of physical parameters that are difficult to measure. However, a simulation study of the transient response of solar cells has not yet been published.

It is the aim of this work to define the domain of validity of the experimental determination of the carrier lifetimes in the base of silicon solar cells and the back surface velocity by using open circuit transient measurements at constant illumination level [referred to as Constant Illumination Open Circuit Voltage Decay (CIOVD) method]. This method, compared to short circuit current methods, is of interest since it offers the possibility of a practical measurement with high carrier concentration conditions. The theory is introduced and a simulation study leads to discuss the accuracy in the determination with regards to the values of technological parameters such as the base doping level and the width of the cell, for application in new solar cell developments.

## EXPERIMENTAL PROCEDURE AND THEORY

The experimental procedure is described in Figure (1). The solar cell is illuminated by means of a uniform steady state photon flux. An abrupt impedance variation obtained by switching off the MOSFET (switching time: 150 ns) at time  $t=0$ , removes rapidly the charge  $R$  and the transient voltage decay is monitored in open circuit conditions. This procedure avoids the ambiguity inherent in carrier injection by electrical pulses [14], removes parasitic impedance effects and enables measurements at any injection level since the illumination remains constant before and during the transient regime.

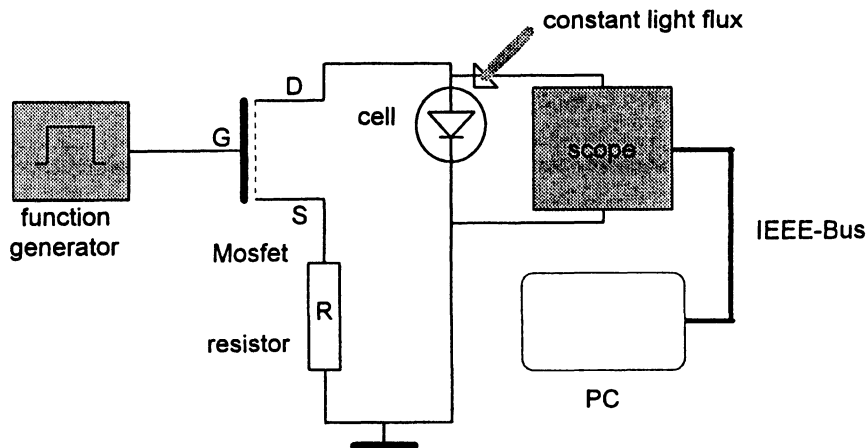


FIGURE 1 Experimental set-up.

In order to analyze the transient voltage, we have to solve the time dependent diffusion equation for the excess minority carrier concentration  $n(x, t)$  in the base region:

$$D \frac{d^2 n(x, t)}{dx^2} + g(x) - \frac{dn(x, t)}{dt} = \frac{n(x, t)}{\tau} + \sum_i U_i \quad (1)$$

including all recombination rates  $U_i$  and the light carrier generation  $g(x)$  (the junction being at  $x=0$  and the back surface at  $x=H$ ),  $D$  is the minority carrier diffusion coefficient. This equation defines the electron lifetime  $\tau$  in the p-type base. The boundary conditions are the open circuit condition:

$$\frac{\partial n(x, t)}{\partial x} \Big|_{x=0} = 0 \quad (t > 0) \quad (2)$$

and the minority carrier recombination condition at the back surface of the cell:

$$\frac{\partial n(x, t)}{\partial x} \Big|_{x=H} = -\frac{S}{D} n(x, t) \Big|_{x=H} \quad (3)$$

which introduces the back surface recombination velocity ( $S$ ). Equation (1), together with the boundary conditions yield the expression of the transient open circuit voltage  $V_{oc}(t)$  at time  $t > 0$  in the form:

$$V_{oc}(t) = V_{oc} - V_T G \sum_{p=0}^{p=\infty} \frac{a_p^2}{D + L^2 w_p^2} e^{-\frac{t}{\tau_p}} \quad (4)$$

where  $G$  is a general characteristic of the cell, defined as:

$$G = d_0 DL \frac{\frac{1}{L} \operatorname{sh}\left(\frac{H}{L}\right) + \frac{S}{D} \operatorname{ch}\left(\frac{H}{L}\right)}{\frac{1}{L} \operatorname{ch}\left(\frac{H}{L}\right) + \frac{S}{D} \operatorname{sh}\left(\frac{H}{L}\right)} \quad (5)$$

The quantities  $d_0$ ,  $a_p$  and  $\tau_p$  are given by:

$$d_0 = 1 - e^{\frac{V_R - V_{oc}}{V_T}} \quad (6)$$

$$a_p^2 = \frac{1}{\frac{H}{2} + \frac{\sqrt{D}}{4w_p} \sin\left(\frac{2w_p H}{\sqrt{D}}\right)} \quad (7)$$

$$\frac{1}{\tau_p} = \frac{1}{\tau} + w_p^2 \quad (8)$$

where the diffusion length  $L$  is given by  $L = (D\tau)^{1/2}$ ,  $V_T$  is the thermal voltage  $kT/q$  ( $k$  is the Boltzmann constant,  $T$  is the absolute temperature and  $q$  is the elementary charge),  $V_{oc}$  is the final open circuit voltage,  $V_R$  is the initial voltage ( $t < 0$ ),  $N_A$  is the base doping concentration and the values of the parameter,  $w_p$ , are the solutions of the transcendental equation:

$$\operatorname{cotg}\left(\frac{w_p H}{\sqrt{D}}\right) = w_p \frac{\sqrt{D}}{S} \quad (9)$$

with  $p\pi \leq w_p H/\sqrt{D} \leq (p+1/2)\pi$ ,  $p$  being an integer  $\geq 0$ . The experimental procedure is deduced from the fact that the series expansion in equation (4) converges uniformly for  $t > 0$  and can be reduced to the first term ( $p = 0$ ) after the initial stage of the decay curve at time  $t \geq t_0$ , which leads to the transient voltage in the form  $V_{oc}(t \geq t_0) = V_{oc} - v_0 \exp(-t/\tau_0)$ . The initial and final voltage  $V_R$  and  $V_{oc}$  are measured and a numerical procedure allows the determinations, at time  $t \geq t_0$ , of the exponential decay time  $\tau_0$  together with the value  $v_0$ . Thus, the parameter value  $w_0$  is determined by equating the numerical value  $v_0$  to the value  $F(w_0)$  of the function  $F(w)$  defined in the restricted interval  $0 \leq w \leq \pi\sqrt{D}/2H$  as follows:

$$F(w) = d_0 V_T \frac{1}{\frac{H}{2} + \frac{\sqrt{D}}{4w} \sin\left(\frac{2wH}{\sqrt{D}}\right)} \frac{DL(w)}{D + w^2 L^2(w)} \frac{\frac{1}{L(w)} \operatorname{sh}\left(\frac{H}{L(w)}\right) + \frac{S}{D} \operatorname{ch}\left(\frac{H}{L(w)}\right)}{\frac{1}{L(w)} \operatorname{ch}\left(\frac{H}{L(w)}\right) + \frac{S}{D} \operatorname{sh}\left(\frac{H}{L(w)}\right)} \quad (10)$$

where

$$L(w) = \frac{\sqrt{D}}{\left(\frac{1}{\tau_0} - w^2\right)^{\frac{1}{2}}} \quad (11)$$

and

$$S = w\sqrt{Dt}g\left(\frac{wH}{\sqrt{D}}\right) \quad (12)$$

The carrier lifetime and the back surface recombination velocity are calculated from equations (8) and (9) where  $p = 0$ .

## SIMULATION

The method starts from a decay curve modelled by equation (4) for simulating an experiment, and applies the experimental procedure to determine the values  $\tau$  and  $S$  of the carrier lifetime and the back surface recombination velocity. These values are compared to the initial input values  $\tau_{in}$  and  $S_{in}$  used to simulate the decay open circuit voltage curve. The technological structure of the silicon solar cell is defined by input parameters which are the base width ( $H$ ) and the base doping level ( $N_A$ ).  $S_{in}$  is supplied directly as a numerical constant. The input carrier lifetime  $\tau_{in}$  ( $\mu\text{s}$ ) and the diffusion coefficient  $D$  ( $\text{cm}^2\text{s}^{-1}$ ) values are given as a function of  $N_A$  ( $\text{cm}^{-3}$ ) by the usual relations:

$$\tau_{in} = \frac{12}{1 + 2N_A 10^{-17}} \quad (13)$$

$$D = V_T \frac{1350}{\left[1 + \frac{81N_A}{N_A + 3.210^{18}}\right]^{\frac{1}{2}}} \quad (14)$$

Due to the rapid decrease of each exponential term of the series expansion [equation (4)], only ten terms are needed to perform the simulation of the decay curve.

Next, our study considers the most relevant structural parameters of the solar cells, namely, doping level of the base  $N_A$  and the base width  $H$ . Three types of silicon cells are of interest here: Classical Thick Cells (CTC,  $H=300 \mu\text{m}$ ), Back Surface Fields cells (BSF,  $H=200 \mu\text{m}$ ) and Optimized Thin Cells (OTC,  $H \approx 50 \mu\text{m}$ ).

## RESULTS

Figure (2) shows the relative variation ( $\delta\tau/\tau = |\tau - \tau_{in}|/\tau$ ) of the determined values of the carrier lifetime as a function of the cell base width for various values of the back surface recombination velocity  $S_{in}$ . Two sets of curves are plotted corresponding to two values of the base doping concentration. The range of these values were used for specifications of high efficiency solar cells. Measurements were performed at time  $t_0 = 1.5 \tau_{in}$ .

A good accuracy ( $\leq 2\%$ ) in the determination of  $\tau$  is obtained for OTC with base doping level greater than  $5 \cdot 10^{16} \text{ cm}^{-3}$  and for BSF and CTC cells with base doping level lower than  $5 \cdot 10^{16} \text{ cm}^{-3}$ . The relative error increases at higher base doping levels (CTC and BSF) as the back surface recombination velocity values decrease. These results show an uncertainty lower than  $0.3 \mu\text{s}$ , which allows one to consider that the method yields, in any case, a good estimate of the carrier lifetime in the cell base. The origin of the upper value, close to 7%, for BSF cells will be discussed below.

The effectiveness of the method in determining the surface recombination velocity  $S$  depends on the ranges of  $S$  values that characterize the technological structure of the solar cell. These ranges are related to the cell base width ( $H$ ) since large values of  $S$  correspond to CTC with a quasi ohmic back contact, whereas small values are required for BSF and OTC where the minority carrier diffusion length exceeds the base thickness. Figures (3), (4) and (5) show typical results obtained for the determination of the surface recombination velocity, for the three types of the

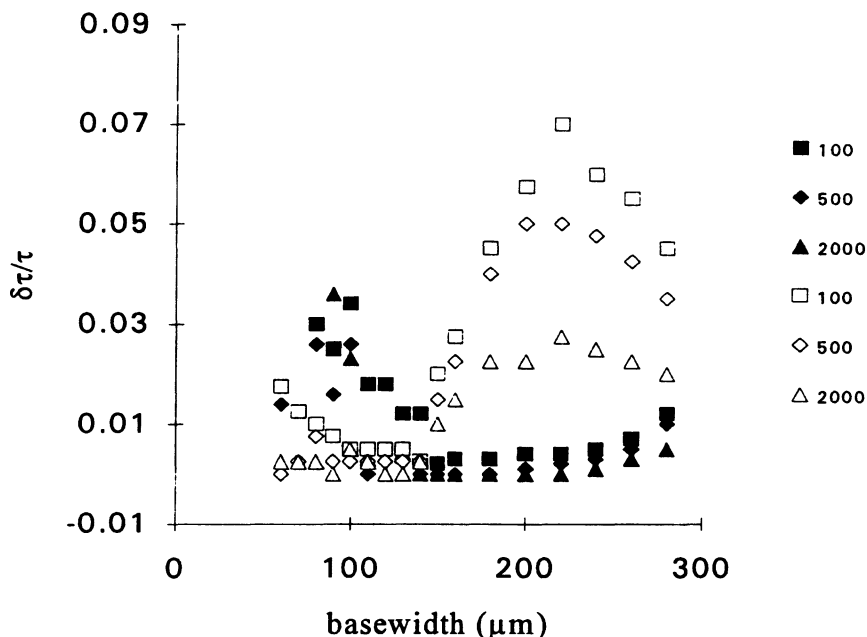


FIGURE 2 Relative error in lifetime  $\tau$  extracted values versus the base width for two doping levels:  $10^{17} \text{ cm}^{-3}$  (open marks) and  $10^{16} \text{ cm}^{-3}$  (solid marks). The input values of the back surface recombination velocity ( $\text{cm.s}^{-1}$ ) are indicated on the right side.

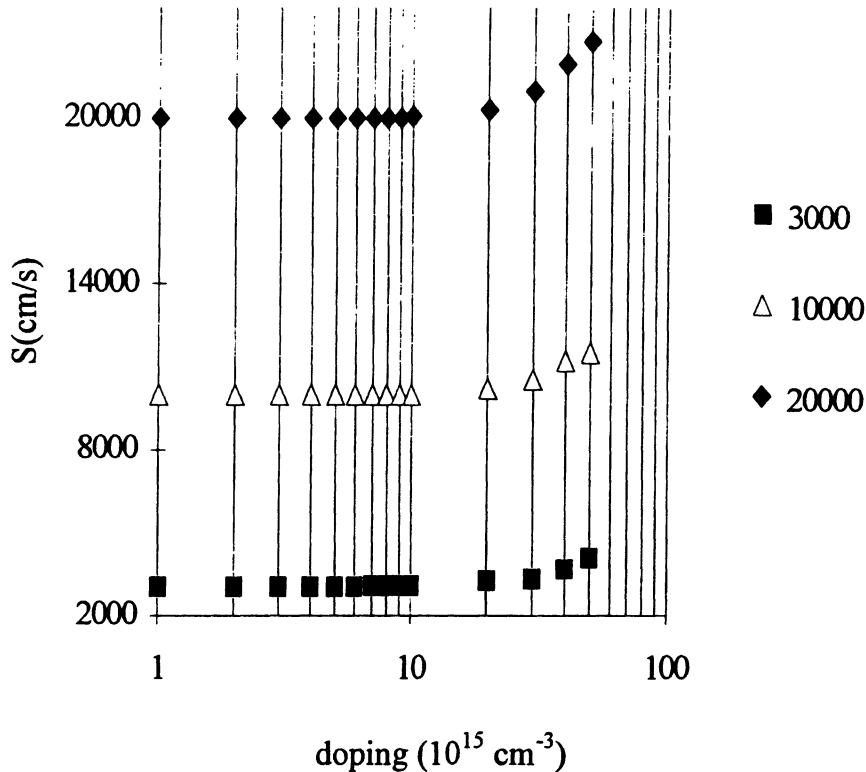


FIGURE 3 Evolution of the extracted back surface recombination velocity values ( $S$ ) with the base doping of thick cells ( $H = 300 \mu\text{m}$ ). The input values  $S_{in}$  ( $\text{cm}\cdot\text{s}^{-1}$ ) are indicated on the right side.

solar cells, as a function of their base doping levels. These figures show that the resolution of the method depends on the doping of the base. For classical thick cells (Fig. (3)) and back surface field cells (Fig. (4)), a good agreement is obtained between measured and input values when doping values are lower than  $3 \cdot 10^{16} \text{ cm}^{-3}$ . The results are less satisfactory for higher doping and the deviation ( $S - S_{in}$ ) increases for  $N_A$  increasing to values for which the minority carrier diffusion lengths become lower than the base width. For these cases, the carrier recombination within the bulk of the base is so high that the cell efficiency is too low for such devices to be produced for solar energy conversion applications.

Regarding OTC, we obtain (Fig. (5)) a good resolution for high base doping level and notable fluctuations and uncertainties as soon as  $N_A$  becomes lower than  $8 \cdot 10^{16} \text{ cm}^{-3}$ . Since it is known [6] that high values of  $N_A$  ( $10^{17} \text{ cm}^{-3}$ ) are required for these structures to obtain maximum output power, the results in Figure (5) show that the transient method is powerful for high efficiency OTC characterizations.

## DISCUSSION

This discussion rests on the practical application of the CIOCVD method for solar cell characterization. In actual situations, the sources of uncertainties affecting the

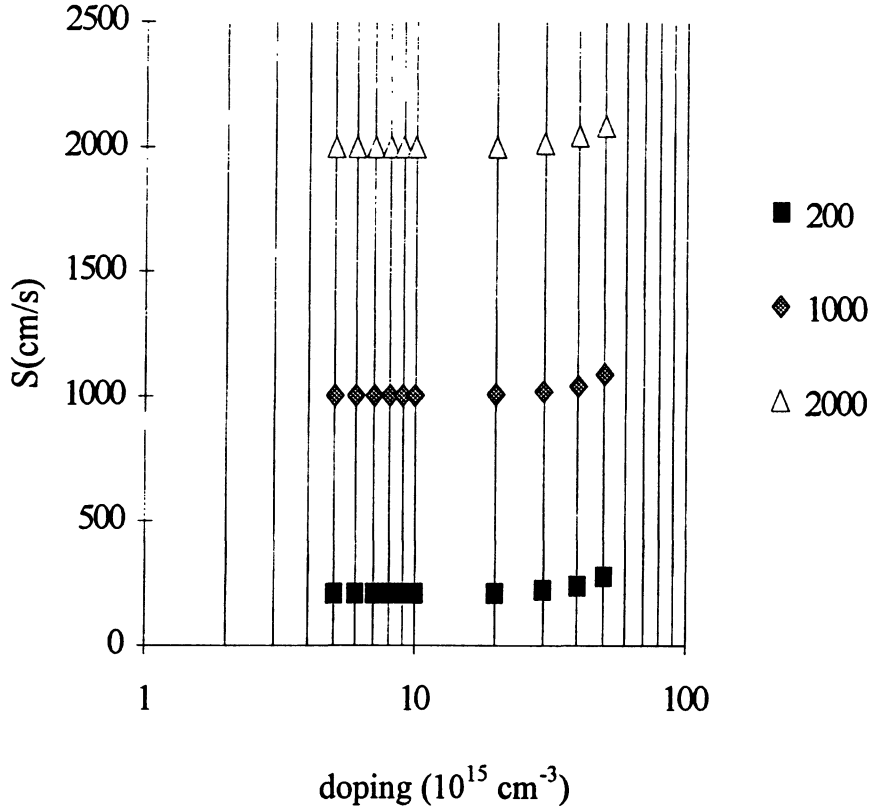


FIGURE 4 Evolution of the extracted back surface recombination velocity values ( $S$ ) with the base doping of BSF cells ( $H = 200 \mu\text{m}$ ). The input values  $S_{\text{in}}$  ( $\text{cm}\cdot\text{s}^{-1}$ ) are indicated on the right side.

determination of  $\tau$  and  $S$  are due to the knowledge of the cell structural parameters ( $H$ ,  $N_A$ ) and on the other side to the evaluation of the time  $t_0$ , which ensures a correct experimental procedure. This knowledge and this evaluation affect the measurements of the three fundamental parameters  $\tau_0$ ,  $w_0$ , and  $v_0$ , which are required for the determination of  $\tau$  and  $S$  using CIOCVD method.

The lifetime value is calculated from the relation  $1/\tau_0 = 1/\tau + w_0^2$ . It is obvious that the contribution due to  $w_0^2$  in this relation is less than  $1/\tau$  value for all practical silicon cell configurations, which implies that the precision of the measurement of  $\tau_0$  is of prime importance. It is obtained as the decay time of the exponential part of the transient open circuit voltage curve, then dependent on the evaluation of the time  $t_0$ . The results presented above show a general agreement between the measured lifetime value  $\tau$  and the input value  $\tau_{\text{in}}$  for all silicon cell configurations, so that the general discussion must be presented all along with the determination of the surface recombination velocity values.

The fundamental assumption is the rapid convergence of the series expansion [equation (4)] in order to describe the decay curve with its first term  $p = 0$ . This can be discussed from results presented in Figures (6) and (7) obtained for the extracted values of  $S$  plotted against the base doping level  $N_A$  for measurements performed at time  $t_0 = \tau_{\text{in}}$  or at  $t_0 = 2\tau_{\text{in}}$ .



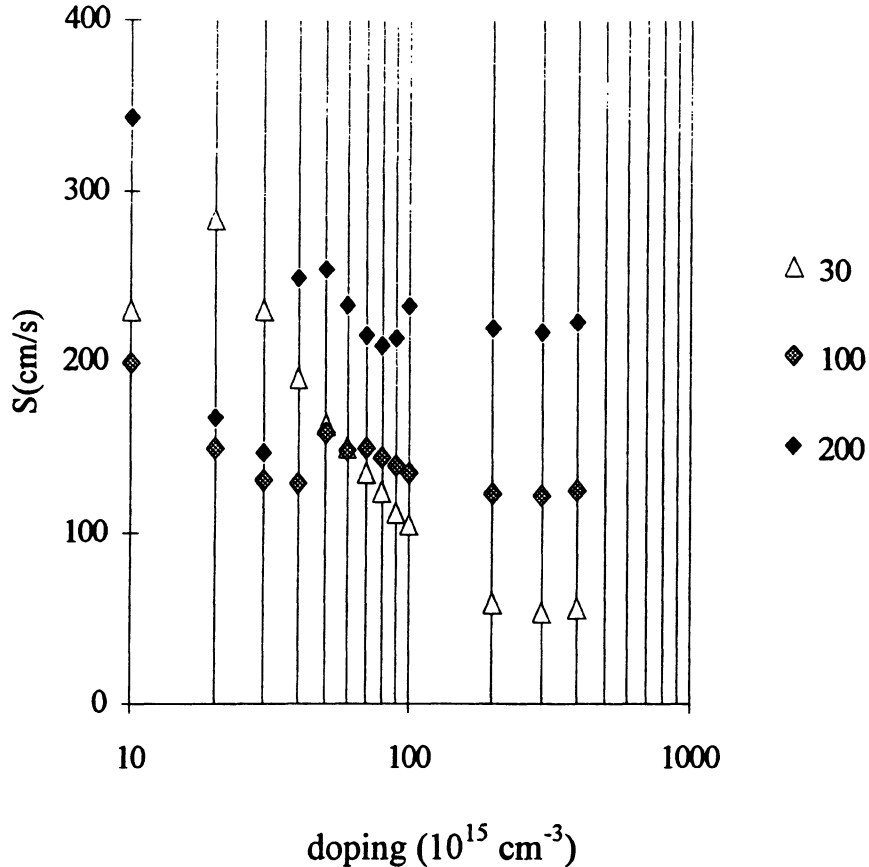


FIGURE 5 Evolution of the extracted back surface recombination velocity values ( $S$ ) with the base doping of optimized thin cells ( $H = 50 \mu\text{m}$ ). The input values  $S_{in}$  ( $\text{cm}\cdot\text{s}^{-1}$ ) are indicated on the right side.

These results point out that at high doping values ( $>4 \cdot 10^{16} \text{ cm}^{-3}$ ) the series convergence decreases with increasing  $N_A$ . The measured  $\tau_0$  values are then greater than the true decay time of the  $p=0$  term, then inducing the observed (Fig. (2)) increase of the uncertainty in the determination of the lifetime for high doping levels and further contributing to produce increase of  $S$  extracted values which has been observed in Figures (3) and (4). It is worth noting that, for specifications of the cell so that the carrier diffusion length is larger than the base width, a very fast convergence of the series expansion is obtained. This is the case for BSF cells with a doping level less than  $3 \cdot 10^{16} \text{ cm}^{-3}$  and an important feature can be seen in Figure (7). In the low doping region, the measurements at time  $t_0 = \tau_{in}$  lead to results better than those obtained at time  $t_0 = 2\tau_{in}$ . In fact, the numerical procedure used to extract  $\tau_0$  indicates that, in such cases, the large decrease of the Signal to Noise ratio yields significant uncertainties in the determination of  $\tau_0$  and of  $v_0$ . This result also accounts for the relative error of 7% found (Fig. (2)) in the determination of  $\tau$  with BSF specifications. Measurements on the asymptotic part of the decay curve are to be avoided.

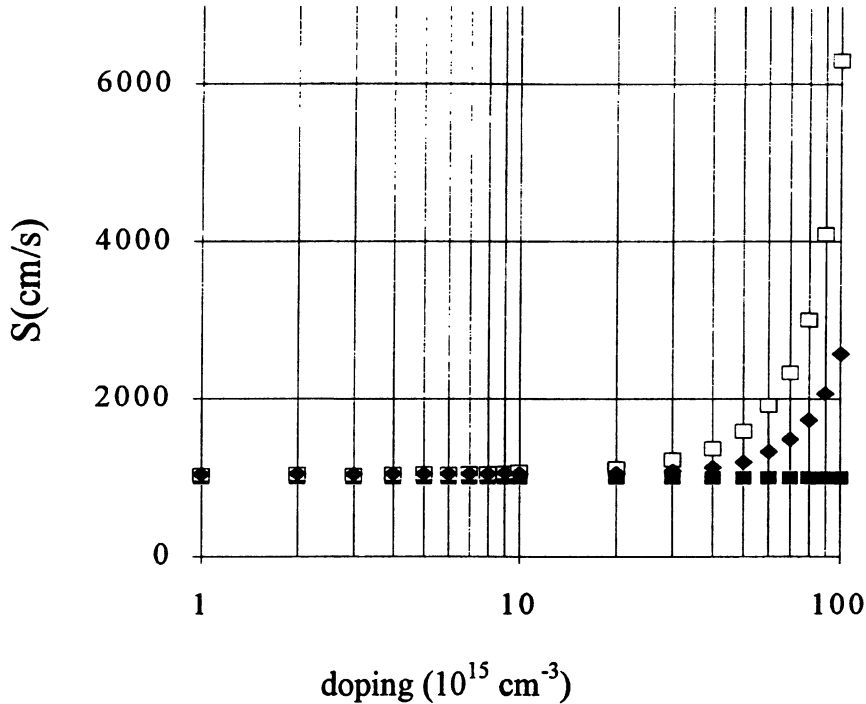


FIGURE 6 Comparison of the extracted back surface recombination values at times  $t_0 = \tau$  (□) and  $t_0 = 2\tau$  (◆) with the input value (■), versus the base doping level of thick cells ( $H = 300 \mu\text{m}$ ),  $S_{\text{in}} = 1000 \text{ cm.s}^{-1}$ .

In order to explain the observed (Fig (3), (4) and (5)) discrepancies between extracted and input values of the surface recombination velocity, two noteworthy features must be taken into account. They concern the determination of the parameter value  $w_0$  arising from the intercept of the graph of the function  $F(w)$  with the horizontal line  $v_0 = \text{constant}$  and the solution of equation (12).

Figures (8) and (9) show the graph of the function  $F(w)$  for different base widths and for two representative values of the input parameter  $S_{\text{in}}$  when  $w$  lies into the restricted interval  $[0, \pi\sqrt{D}/2H]$ . The first noteworthy feature is that the difference between the lower and the upper limits of the function  $F(w)$  decreases as  $H$ ,  $S$  and  $N_A$  decrease.

These figures show that the intercept with any straight line  $v_0 = \text{constant}$  is well defined for  $H=300 \mu\text{m}$  but difficult to be obtained for  $H = 50 \mu\text{m}$ , which provide large uncertainties in  $w_0$  values having contributed to the fluctuations observed in Figure (5). The values of the initial and final voltages appear through the difference  $V_R - V_{\text{oc}}$  and affect the range of variation of  $F(w)$  as well. This effect is only apparent for high illumination levels of high efficiency solar cells where a large variation of the output current is produced by a small variation of the applied voltage around the open circuit voltage value.

The second noteworthy feature lies in the observation (Fig. (10)) of the great dispersion of  $S$  values within a small range of  $w$  values for  $S < 300 \text{ cm.s}^{-1}$  as well as

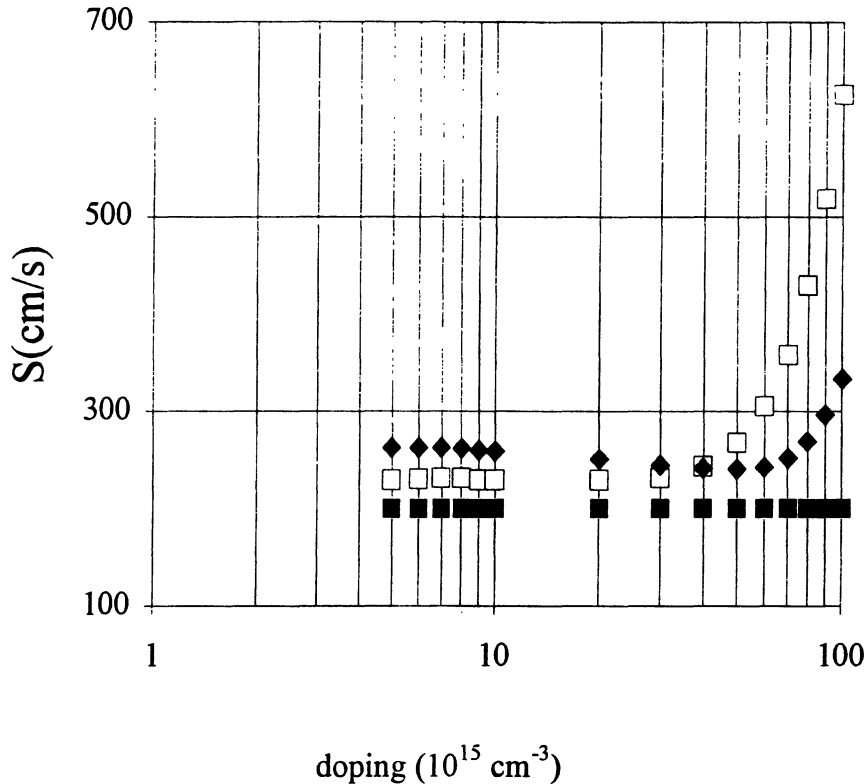


FIGURE 7 Comparison of the extracted back surface recombination values at times  $t_0 = \tau$  ( $\square$ ) and  $t_0 = 2\tau$  ( $\blacklozenge$ ) with the input value ( $\blacksquare$ ), versus the base doping level of BSF cells ( $H = 200 \mu\text{m}$ ),  $S_{\text{in}} = 200 \text{ cm}\cdot\text{s}^{-1}$ .

for  $S > 1000 \text{ cm}\cdot\text{s}^{-1}$ . This implies a poor accuracy in the determination of low and high values of the recombination velocity which has been observed in Figures (3) and (5) and discussed above.

The general discussion of the determination of the back surface recombination velocity obtained with CIOCVD method shows that the precision depends on the specification of each type of solar cell structure. It leads to a correct extraction of the parameters when the optimization of the determination of  $\tau_0$  with regard to time  $t_0$  is taken into account.

## CONCLUSION

The open circuit voltage decay method using a constant illumination level for extracting the bulk lifetime and the rear surface recombination velocity in solar cells has been investigated in view of applications to thin and thick silicon solar cell developments. The determination of three parameters is needed and it is shown that the precision of the extracted values of  $\tau$  and  $S$  are related to the structure of the solar cells and to the method.

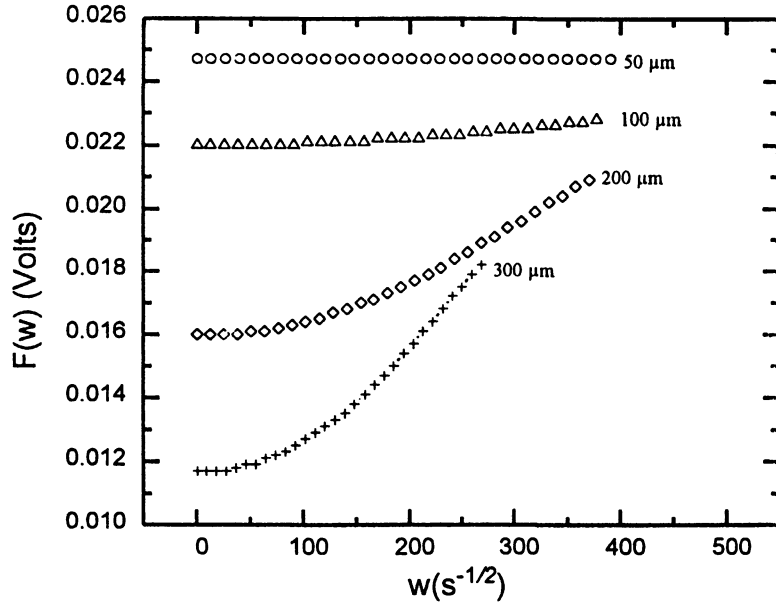


FIGURE 8 Plots of the function  $F(w)$  for various values of cell base width ( $H$ ),  $w$  lying into the restricted interval  $[0, \pi\sqrt{D}/2H]$ . Input value of the back surface velocity:  $100 \text{ cm}\cdot\text{s}^{-1}$ ; doping level value:  $3 \cdot 10^{16} \text{ cm}^{-3}$ .

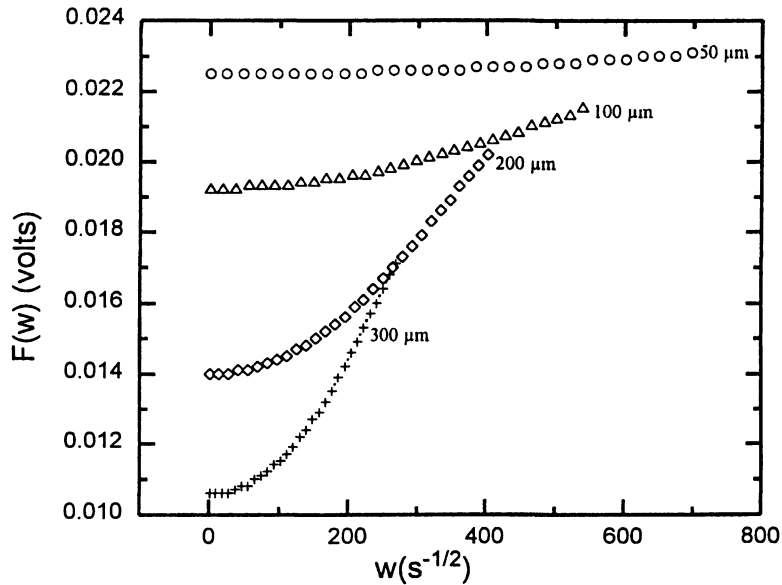


FIGURE 9 Plots of the function  $F(w)$  for various values of cell base width ( $H$ ),  $w$  lying into the restricted interval  $[0, \pi\sqrt{D}/2H]$ . Input value of the back surface velocity:  $2000 \text{ cm}\cdot\text{s}^{-1}$ ; doping level value:  $3 \cdot 10^{16} \text{ cm}^{-3}$ .

Deviations in the extracted lifetime values lie within 7% and increase with increasing base doping levels for structures characterized by low values of the back surface recombination velocity. A proper determination is needed to ensure that the calculated part of the exponential decay is not influenced by higher decay modes while maintaining signal-to-noise ratio sufficiently high. Simulation of the decay curve confirms experimental errors in the determination of the decay time constant when the measurements are performed in the asymptotic part of the decay curve.

For high values of  $S$  (thick cells), resolution in the determination of the back surface recombination velocity decreases with increasing base doping level and for the case of low base doping levels of thin cells with decreasing  $S$  values. Our simulation study shows that such a resolution is related to the method when applied to low efficiency solar cell structures.

The CIOCV method is a valuable tool for solar cell characterization which eliminates the parasitic impedance effects and allows the measurements of the carrier lifetime and the back surface recombination velocity with operating effective illumination of the solar cell.

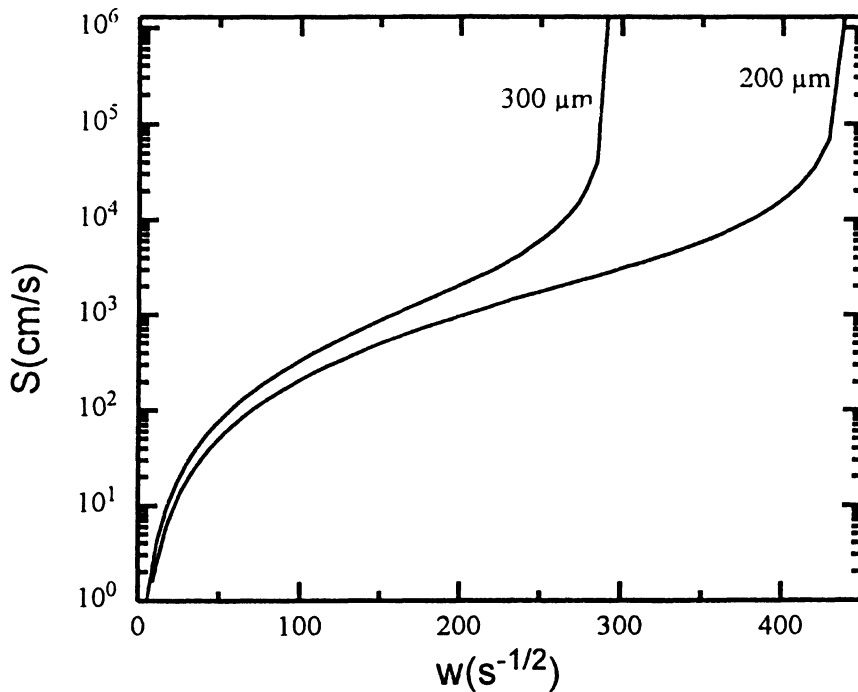


FIGURE 10 The back surface recombination velocity as a function of  $w$ , parameter lying into the restricted interval  $[0, \pi\sqrt{D}/2H]$ , for two values of the base width. The base doping of the cell is  $10^{16} \text{ cm}^{-3}$ .

## REFERENCES

1. J.H. Werner, S. Kolodinski, U. Rau, J. Arch and E. Bauser, *Appl. Phys. Lett.*, **62**, 2998–3000 (1993).
2. J.C. Minano, A. Luque, I. Tobias, *Appl. Optics*, **31**, 3114–22 (1992).
3. A.G. Aberle, G. Heiser and M. Green, *J. Appl. Phys.*, **75**, 5391–405 (1994).
4. P. Mialhe, B. Affour, K. El-Hajj and A. Koury, *Active and Passive Elec. Comp.*, **17**, 227–32 (1995).
5. F. Pelanchon and P. Mialhe, *Solid State Electron.*, **33**, 47–51 (1990).
6. F. Pelanchon, S. Mouhammad and P. Mialhe, *Renewable Energy*, **2**, 645–48 (1992).
7. Z.G. Ling, P.K. Ajmera and G.S. Kousik, *J. Appl. Phys.*, **75**, 2718–20 (1994).
8. S.R. Dhariwal and N.K. Vasu, *Solid State Electron.*, **24**, 915–27 (1981).
9. P. Mialhe, G. Sissoko and M. Kane, *J. Appl. Phys.*, **20**, 762–765 (1987).
10. K. Joardar, R.C. Ondero and D.K. Schroder, *Solid State Electron.*, **32**, 479–483 (1989).
11. K. Burgard, W. Schmidt, W. Warta, *Solar Energy Materials and Solar Cells*, **36**, 241–59 (1995).
12. J.M. Salagnon, S. Mouhammad, P. Mialhe and F. Pelanchon, *Solar Cells*, **31**, 223–36 (1991).
13. P. Mialhe, G. Sissoko, F. Pelanchon and J.M. Salagnon, *J. Phys. III*, **2**, 2317–31 (1992).
14. T. Jung, F.A. Lindholm and A. Neugroshel, *Solar Cells*, **22**, 81–96 (1987).